














RESEARCH ARTICLE | AUGUST 22 2024

# Development of fast 2.5 MeV neutron detectors for high-intensity stray magnetic field environments

Special Collection: [Proceedings of the 25th Topical Conference on High-Temperature Plasma Diagnostics](#)



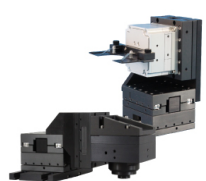
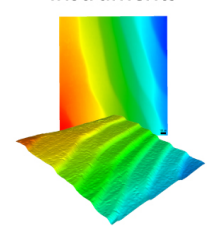
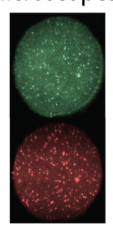
A. Dal Molin ; F. Guiotto ; O. Putignano ; M. Dalla Rosa ; P. Franz ; G. Grosso ; A. Monguzzi ; E. Perelli Cippo ; L. Pollice ; D. Rigamonti ; L. G. Tedoldi ; M. Zuin ; M. Tardocchi 



Rev. Sci. Instrum. 95, 083544 (2024)

<https://doi.org/10.1063/5.0219121>



|  |  |  |   |  |
|--|--|--|---|--|
|  <p><b>MCL</b><br/>MAD CITY LABS INC.<br/>www.madcitylabs.com</p> | <p>Nanopositioning Systems</p>  | <p>Modular Motion Control</p>  | <p>AFM and NSOM Instruments</p>  | <p>Single Molecule Microscopes</p>  |
|--|--|--|---|--|

# Development of fast 2.5 MeV neutron detectors for high-intensity stray magnetic field environments

Cite as: Rev. Sci. Instrum. 95, 083544 (2024); doi: 10.1063/5.0219121

Submitted: 15 May 2024 • Accepted: 7 August 2024 •

Published Online: 22 August 2024



View Online



Export Citation



CrossMark

A. Dal Molin,<sup>1,a)</sup> F. Guiotto,<sup>2,4</sup> O. Putignano,<sup>1</sup> M. Dalla Rosa,<sup>3</sup> P. Franz,<sup>4</sup> G. Grosso,<sup>1</sup> A. Monguzzi,<sup>5</sup> E. Perelli Cippo,<sup>1</sup> L. Pollice,<sup>5</sup> D. Rigamonti,<sup>1</sup> L. G. Tedoldi,<sup>3</sup> M. Zuin,<sup>4,6</sup> and M. Tardocchi<sup>1</sup>

## AFFILIATIONS

<sup>1</sup>Istituto per la Scienza e Tecnologia dei Plasmi, CNR, Milan, Italy

<sup>2</sup>Università degli Studi di Padova - Centro Ricerche Fusione (CRF), Padua, Italy

<sup>3</sup>Università degli Studi di Milano-Bicocca, Dipartimento di Fisica, Milan, Italy

<sup>4</sup>Consorzio RFX, Padua, Italy

<sup>5</sup>Università degli Studi di Milano-Bicocca, Dipartimento di Scienze dei Materiali, Milan, Italy

<sup>6</sup>Istituto per la Scienza e Tecnologia dei Plasmi, CNR, Padua, Italy

**Note:** This paper is part of the Special Topic on Proceedings of the 25th Topical Conference on High-Temperature Plasma Diagnostics.

**a)** Author to whom correspondence should be addressed: [andrea.dalmolin@istp.cnr.it](mailto:andrea.dalmolin@istp.cnr.it)

## ABSTRACT

Several small to medium-scale magnetic confinement fusion devices operate using deuterium as fuel. These low neutron rate ( $10^8$ – $10^{10}$  n/s) devices rely on 2.45 MeV neutron measurements to validate physical models and to assess their performance. Given the modest rate, neutron monitors have to be placed as close as possible to the machine to maximize data gathering. In these regions, intense stray magnetic fields could affect the detector's performance. In this work, the development of a neutron detector based on an EJ-276D scintillator crystal coupled with a SiPM and a custom-made readout system is presented. The detector has particle discrimination capability and is insensitive to magnetic fields.

© 2024 Author(s). All article content, except where otherwise noted, is licensed under a Creative Commons Attribution-NonCommercial-NoDerivs 4.0 International (CC BY-NC-ND) license (<https://creativecommons.org/licenses/by-nc-nd/4.0/>). <https://doi.org/10.1063/5.0219121>

## I. INTRODUCTION

Recent fusion breakthroughs<sup>1–3</sup> accelerated interest in the field for both public and private investors. Several new experimental devices are being proposed and built while existing experiments are being expanded and upgraded.<sup>4</sup> Small to medium-scale magnetic confinement fusion devices commonly operate using deuterium as fuel. This choice allows for the validation of plasma models and the capability of sustaining nuclear reactions, avoiding the complication of tritium handling.

Neutron measurements are crucial, as they provide valuable insights into the yield and allow exploration of various nuclear regimes. The state-of-the-art technique adopted at magnetic

confinement fusion devices for 2.45 MeV neutron measurement is based on the time-of-flight (TOF) technique.<sup>5</sup> Such large and expensive diagnostic systems are best suited for high neutron rate devices (over  $10^{16}$  n/s) where operation under high counting rates is expected. In numerous small to medium-scale applications, the neutron rates involved fall within the range of  $10^8$ – $10^{10}$  neutrons per second. For these applications, the most sensible type of neutron detector is based on a scintillator coupled with a photodetector.<sup>6</sup>

Given these moderate rates, it is imperative to position the detectors as close to the machine as possible to maximize the detection statistics. This region of the devices often presents intense stray magnetic fields on the order of hundreds of mT that could affect the behavior of the detector. To ensure the accuracy and reliability of the

neutron measurements while avoiding the use of extensive magnetic shielding, a detector insensitive to these stray magnetic fields must be developed.

In this contribution, we present the development of a fast neutron detector optimized for the measurement of deuterium–deuterium 2.45 MeV neutrons in high-intensity stray magnetic fields with neutron-to-gamma discrimination capability for the RFX-mod2 device.<sup>4</sup> Solutions akin to the one outlined in this contribution could be potentially employed in other deuterium-fueled machines with high-intensity stray fields.

## II. METHODS

Some scintillator materials, such as EJ-276D, CLYC, or LaCl<sub>3</sub>:Ce, can be used to discriminate against different kinds of interacting particles by studying the fast ( $\tau_f$ ) and slow ( $\tau_s$ ) components of the scintillation light. These scintillators are preferred for this application for their ability to discriminate neutrons against the gamma ray background. Chlorine-based scintillators possess a peaked response function to neutrons due to the  $^{35}\text{Cl}(n,p)^{35}\text{S}$  reaction. This characteristic response is optimal for performing neutron spectroscopy.<sup>7,8</sup> However, the  $^{35}\text{Cl}(n,p)^{35}\text{S}$  reaction cross section for 2.45 MeV neutrons is approximately one order of magnitude lower than the interaction with carbon or hydrogen. As a consequence, the detection efficiency for a 1'' long LaCl<sub>3</sub>:Ce or CLYC crystal is  $\sim 35$  times lower than for an EJ-276D. This lower detection efficiency is not ideal for low neutron rate scenarios. For this reason, EJ-276D was selected as the scintillator crystal for this application.

Photomultiplier tubes (PMTs) are the most sensitive detector components to intense stray magnetic fields, as they can even be affected by Earth's magnetic field ( $\sim 0.05$  mT).<sup>9</sup> In the presence of magnetic fields of several hundreds of mT, such as those found near the vessel of magnetic confinement fusion devices, several kilograms of magnetic shielding material are necessary to avoid gain shift and to guarantee the correct detector performance. This design choice increases the diagnostic cost and the occupied volume while increasing engineering and manufacturing challenges.

Silicon Photomultipliers (SiPMs) are insensitive to magnetic fields and could be used to replace PMTs as the photodetector component of the diagnostic. In addition, SiPMs are smaller than PMTs, leading to a more compact detector. On the other hand, SiPM gain can substantially change with temperature, and their response can be non-linear depending on the signal energy and rate. Dedicated solutions to these drawbacks were already investigated and presented in previous studies.<sup>10,11</sup>

The use of SiPMs as photodetectors could introduce another complication in the design. Compared to PMTs, SiPMs possess a slower characteristic time response that could affect or prevent particle discrimination based on scintillation timing.<sup>12</sup> To address this issue, the SiPM characteristic time was compensated using a dedicated pole-zero readout circuit, restoring discrimination capability while avoiding significant loss in signal amplitude and undershooting.

The pole-zero cancellation circuit consists of passive components (a capacitor and two resistors) designed to counteract the slow time response introduced by the SiPM's characteristic time in the detector's transfer function. This is achieved by introducing a

zero at the same location in the Laplace transform space, effectively canceling out the undesirable pole.

The main aim of this work is to test the particle discrimination capability for a novel neutron detector insensitive to magnetic fields. The detector was comprised of a  $15 \times 25$  mm<sup>2</sup> EJ-276D fast plastic scintillator coupled with a Hamamatsu S13361-3050NE-04 silicon photomultiplier and a custom-made readout system with a dedicated pole-zero cancellation circuit (Fig. 1).

Different gamma ray calibration sources ( $^{22}\text{Na}$ ,  $^{60}\text{Co}$ ,  $^{137}\text{Cs}$ , and  $^{152}\text{Eu}$ ) were used to calibrate the detector response in energy. Figure 2 shows the resulting calibrated spectra. To compare energy deposition in the detector regardless of the type of particle, all light outputs are expressed in units of mega electron volt electron equivalent (MeVee).

The Compton effect is the main gamma-ray interaction with the EJ-276D plastic scintillator. The resulting Compton edges ( $E_C$ , indicated by arrows in the figure) depend on the radioactive source monoenergetic gamma-ray energy ( $E_0$ ) through the relation

$$E_C = E_0 \left( 1 - \frac{1}{1 + \frac{2E_0}{m_e c^2}} \right),$$

where  $m_e$  is the electron rest mass and  $c$  is the speed of light in a vacuum.

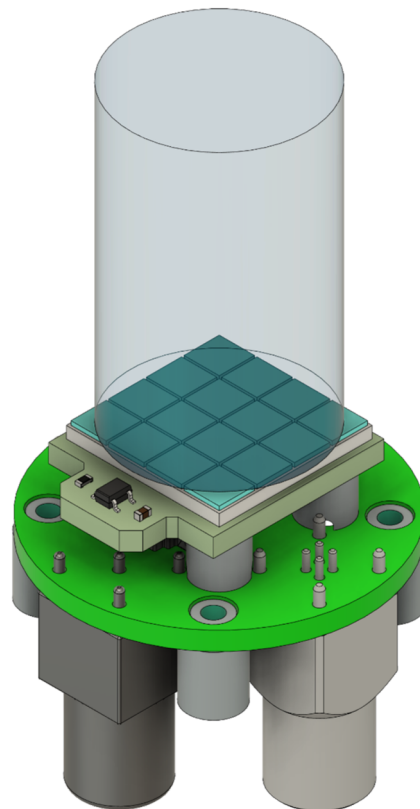
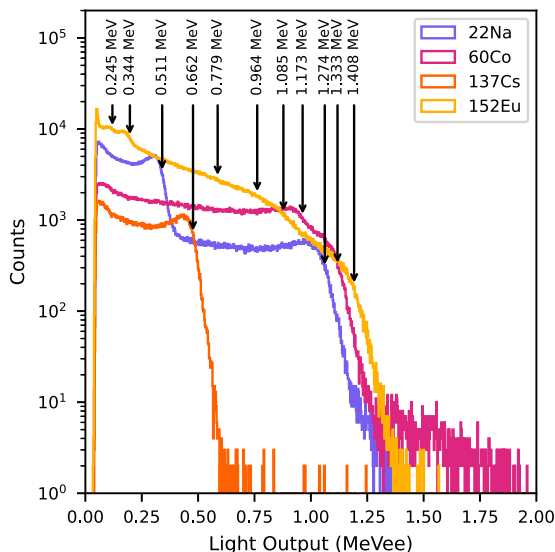
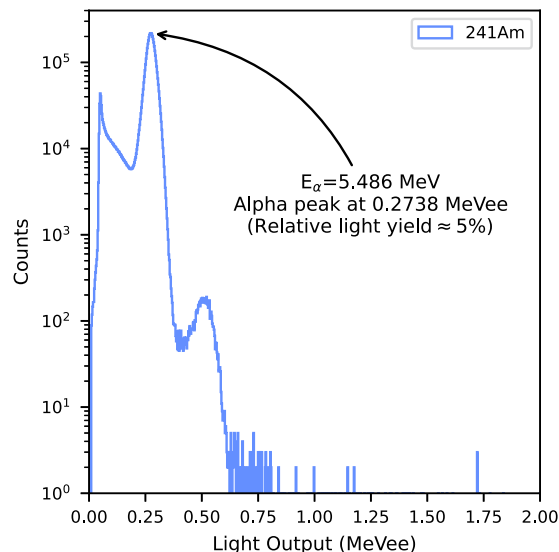


FIG. 1. A schematic of the detector design. From top to bottom: the scintillator crystal, the silicon photomultiplier with the temperature sensor, and the custom-made readout base with the pole-zero cancellation circuit.



**FIG. 2.** Energy spectra of different gamma-ray sources used for calibration. Compton edges for the corresponding monoenergetic gamma emission are marked with arrows.



**FIG. 4.** Energy spectrum of an alpha particle source calibrated using known gamma ray sources.

Compton edges were identified using the second finite differences of adjacent bin counts. Error function fitting of the Compton edge was then used to improve accuracy. Compton edges presented an excellent linear relation with their position in analog-to-digital converter (ADC) channels. The fitted calibration line is shown as a dashed line in Fig. 3.

Particle discrimination was tested using an alpha particle source ( $^{241}\text{Am}$ ). The alpha source was placed in direct contact with

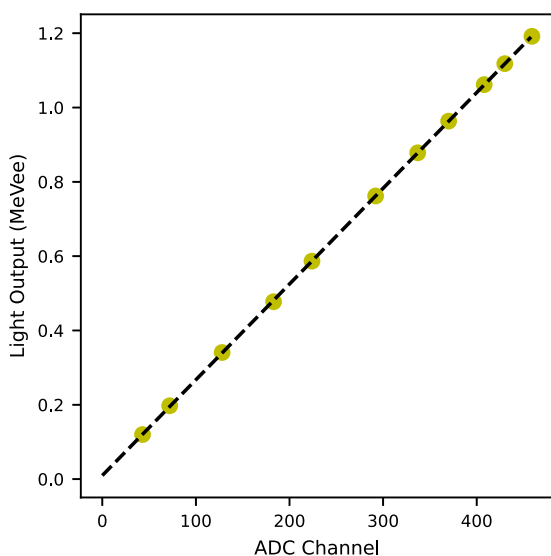


**FIG. 3.** Calibration of the EJ-276D detector. Compton edges for known calibration gamma ray sources are represented by the yellow dots. The black dashed line is the fitted linear calibration.

the crystal to avoid air attenuation. The measured spectrum is shown in Fig. 4.

In the alpha spectrum, two peaks are visible. One peak is centered at 0.2738 MeVee, and it is due to the  $^{241}\text{Am}$  5.486 MeV alpha interaction with the scintillator crystal. The difference in interaction with the scintillator between alpha particles and gamma rays causes a relatively reduced emission of scintillation photons for the former. The measured light yield of alpha particles, when compared to gamma rays, is  $\sim 5\%$ . The second peak, centered around 0.5 MeVee, is approximately three orders of magnitude less intense than the one centered at 0.2738 MeVee and will be discussed in Sec. III.

### III. RESULTS

Event waveforms were collected for each of the measured radioactive sources. An analysis of the fast ( $\tau_f$ ) and slow ( $\tau_s$ ) signal components was performed by fitting a double exponential decay to an average of 100 energy-equivalent pulses for both gamma ray and alpha particle signals. Results are shown in Fig. 5.

The gamma ray fast component for the measured waveforms is  $\tau_f = (20.7 \pm 0.1)$  ns, while the slow component is  $\tau_s = (340.0 \pm 20.0)$  ns. For alpha particles, the fast component is  $\tau_f = (25.0 \pm 0.2)$  ns, while the slow component is  $\tau_s = (420.0 \pm 9.0)$  ns. The gamma ray signal is faster than the alpha, both in its fast and slow components. More importantly, gamma ray and alpha particle signals possess statistically different fast and slow components, proving that particle discrimination capability was restored by using the pole-zero compensation circuit.

Pulse fitting is a computationally expensive and slow analysis that can only be performed off-line. An alternative, real-time analysis that allows for particle discrimination is based on differential gating. In this technique, particle discrimination is achieved by comparing the signal integrated over a short ( $Q_s$ ) and a long ( $Q_l$ )

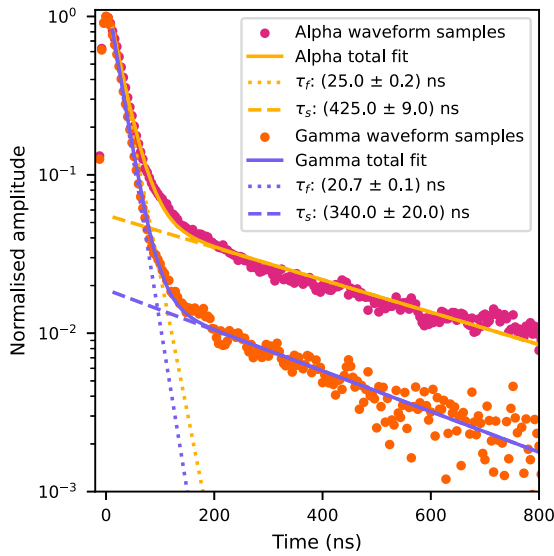


**FIG. 5.** Pulse shape comparison between an alpha particle and a gamma-ray signal. Each of the two waveforms is the result of an average of 100 equivalent pulses.

time window. The pulse shape discrimination (PSD) value is then computed for each event as

$$PSD = \frac{Q_l - Q_s}{Q_l} \approx \frac{\text{Tail contribution}}{\text{Total signal}}.$$

A 2D histogram containing the PSD and light output of the measured events is shown in Fig. 6.

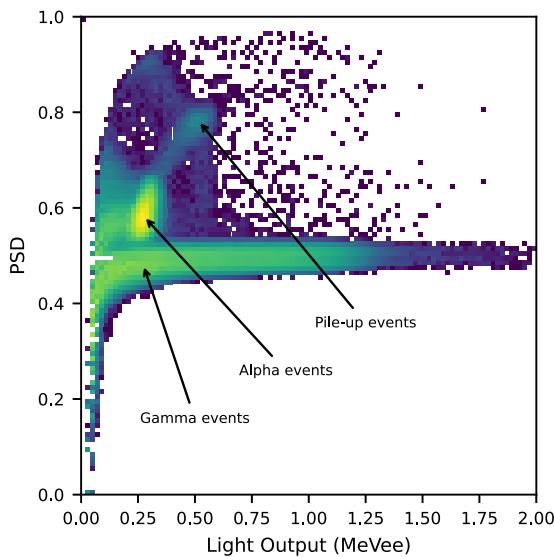


**FIG. 6.** Pulse shape discrimination histogram. The three regions corresponding to gamma-ray, alpha particle, and pile-up events are highlighted.

In the 2D histogram, gamma ray events can be identified against alpha particle events due to their lower tail (slow) contribution to the total signal ( $PSD < 0.55$ ). Alpha particle events are clustered around the peak at 0.2738 MeVee with an average PSD value of 0.6. Using a threshold of 0.2 MeVee, the figure of merit for alpha-to-gamma ray discrimination is equal to 0.99. Finally, the secondary peak identified in Fig. 4 centered at 0.5 MeVee can now be attributed to pile-up events. The high PSD value ( $\sim 0.8$ ) suggests a second pile-up event on the tail of the primary waveform. This suggestion is confirmed by inspection of the waveforms belonging to this region of the 2D histogram.

For low counting rate applications, such as the one presented in this work, pile-up should not represent a significant issue. If necessary, pile-up can be appropriately addressed using pulse shape analysis based on waveform fitting during off-line analysis.

Figure 6 demonstrates that particle discrimination with SiPMs can be achieved even for more crude, real-time analysis based on differential gating.

#### IV. CONCLUSION

This study showed that the inherent pulse shape discrimination capability found in some scintillator crystals, particularly EJ-276D, can be preserved even when coupled with Silicon Photomultipliers (SiPMs). By using SiPMs as photosensors, it becomes possible to craft neutron detectors that are compact and insensitive to magnetic fields.

Neutrons are detected through their scattering with protons in the scintillation material, which have a lower stopping power compared to alpha particles. As a result, neutron-to-gamma discrimination is expected to be more challenging than the alpha-to-gamma discrimination discussed in this work. If these initial results are confirmed in future experiments with a fast neutron source, this technological advancement will pave the way for the development of robust and adaptable detection systems capable of operating efficiently in diverse environmental conditions. These neutron detectors could be deployed near the vessel of magnetic confinement fusion devices to maximize data collection and increase statistics and time resolution. Moreover, the use of a more compact photodetector and the lack of requirement for magnetic shielding open up the possibility of using an array of detectors to investigate multiple lines of sight.

Future applications of this work are foreseen to be adopted at small and medium-scale devices like RFX-mod2, to provide spatial and time-resolved 2.45 MeV neutron measurement of the deuterium reaction and to investigate neutron production during magnetic reconnection events.<sup>13</sup>

#### ACKNOWLEDGMENTS

This work has been carried out within the framework of the Italian National Recovery and Resilience Plan (NRRP), funded by the European Union—NextGenerationEU (Mission 4, Component 2, Investment 3.1—Area ESFRI Energy—Call for Tender No. 3264 of 28-12-2021 of the Italian University and Research Ministry (MUR), Project ID IR0000007, MUR Concession Decree No. 243 del 04/08/2022, CUP B53C22003070006, “NEFERTARI—New

Equipment for Fusion Experimental Research and Technological Advancements with RFX Infrastructure”). Views and opinions expressed are, however, those of the authors only and do not necessarily reflect those of the European Union or the European Commission. Neither the European Union nor the European Commission can be held responsible for them.

## AUTHOR DECLARATIONS

### Conflict of Interest

The authors have no conflicts to disclose.

### Author Contributions

**A. Dal Molin:** Conceptualization (equal); Data curation (equal); Formal analysis (equal); Investigation (equal); Methodology (equal); Software (equal); Supervision (equal); Validation (equal); Writing – original draft (equal); Writing – review & editing (equal). **F. Guiotto:** Investigation (equal). **O. Putignano:** Investigation (equal); Visualization (equal). **M. Dalla Rosa:** Formal analysis (equal); Investigation (equal). **P. Franz:** Investigation (equal). **G. Grosso:** Conceptualization (equal); Investigation (equal); Methodology (equal); Resources (equal); Supervision (equal). **A. Monguzzi:** Conceptualization (equal); Methodology (equal); Resources (equal). **E. Perelli Cippo:** Conceptualization (equal); Investigation (equal). **L. Pollice:** Investigation (equal). **D. Rigamonti:** Conceptualization (equal); Investigation (equal); Methodology (equal); Validation (equal); Writing – review & editing (equal). **L. G. Tedoldi:** Data curation (equal); Formal analysis (equal); Investigation (equal); Visualization (equal). **M. Zuin:** Conceptualization (equal); Funding acquisition (equal); Resources (equal); Supervision (equal); Validation (equal). **M. Tardocchi:** Funding acquisition (equal); Project administration (equal); Resources (equal); Supervision (equal); Visualization (equal).

### DATA AVAILABILITY

The data that support the findings of this study are available from the corresponding author upon reasonable request.

### REFERENCES

<sup>1</sup>H. Abu-Shawareb *et al.*, “Lawson criterion for ignition exceeded in an inertial fusion experiment,” *Phys. Rev. Lett.* **129**, 075001 (2022).

<sup>2</sup>A. B. Zylstra *et al.*, “Burning plasma achieved in inertial fusion,” *Nature* **601**, 542–548 (2022).

<sup>3</sup>C. Maggi, “Foreword to the nuclear fusion special issue of papers presenting results from the JET tritium and deuterium/tritium campaign,” *Nucl. Fusion* **63**, 110201 (2023).

<sup>4</sup>S. Peruzzo, D. Aprile, M. Dalla Palma, M. Pavei, D. Rizzetto, A. Rizzolo, D. Abate, P. Agostinetti, M. Agostini, R. Andreani, F. Anselmi, F. Battistin, A. Bernardi, M. Bernardi, G. Berton, P. Bettini, M. A. Bigi, M. Bonotto, M. Brombin, A. Canton, L. Carraro, R. Cavazzana, L. Cordaro, G. Corniani, S. Dal Bello, A. De Lorenzi, G. De Masi, F. Degli Agostini, L. Franchin, P. Franz, G. Gambetta, F. Gnesotto, L. Grando, P. Innocente, B. Laterza, L. Lotto, S. Manfrin, G. Marchiori, N. Marconato, D. Marcuzzi, L. Marrelli, E. Martines, M. Moresco, A. Novella, P. Piovani, N. Pomaro, F. Rossetto, M. Siragusa, P. Sonato, S. Spagnolo, M. Spolaore, C. Talerjercio, D. Terranova, A. Tiso, L. Trevisan, M. Valente, M. Valisa, M. Zaupa, and M. Zuin, “The new vessel complex for the RFX-mod2 experiment: An effective synergy between fusion research and technological development,” *Fusion Eng. Des.* **194**, 113890 (2023).

<sup>5</sup>M. Gatun Johnson, L. Giacomelli, A. Hjalmarsson, J. Källne, M. Weiszflog, E. Andersson Sundén, S. Conroy, G. Ericsson, C. Hellesen, E. Ronchi, H. Sjöstrand, G. Gorini, M. Tardocchi, A. Combo, N. Cruz, J. Sousa, and S. Popovichev, “The 2.5-MeV neutron time-of-flight spectrometer TOFOR for experiments at JET,” *Nucl. Instrum. Methods Phys. Res., Sect. A* **591**, 417–430 (2008).

<sup>6</sup>L. Giacomelli, A. Zimbal, K. Tittelmeier, H. Schuhmacher, G. Tardini, and R. Neu, “The compact neutron spectrometer at ASDEX Upgrade,” *Rev. Sci. Instrum.* **82**, 123504 (2011).

<sup>7</sup>M. Nocente *et al.*, “COSMONAUT: A COmpact spectrometer for measurements of neutrons at the ASDEX upgrade tokamak” (these proceedings) (2024).

<sup>8</sup>D. Rigamonti *et al.*, “A Chlorine based scintillator (LaCl<sub>3</sub>) for 2.5 MeV neutron spectroscopy in deuterium nuclear fusion plasmas” (these proceedings) (2024).

<sup>9</sup>R. M. Faradzhaev, Y. A. Trofimov, E. E. Lupar, and V. N. Yurov, “Performances investigation and material selection of PMT magnetic shields for the space experiments with GRIS and PING-M instruments,” *J. Phys.: Conf. Ser.* **675**, 042008 (2016).

<sup>10</sup>A. Dal Molin, L. Fumagalli, M. Nocente, D. Rigamonti, M. Tardocchi, L. Giacomelli, E. Panontin, A. Lvovskiy, C. Paz-Soldan, N. W. Edietis, and G. Gorini, “Novel compact hard x-ray spectrometer with MCps counting rate capabilities for runaway electron measurements on DIII-D,” *Rev. Sci. Instrum.* **92**, 043517 (2021).

<sup>11</sup>A. Lvovskiy, C. Paz-Soldan, N. Eidiets, A. Dal Molin, M. Nocente, C. Cooper, D. Rigamonti, M. Tardocchi, and D. Taussig, “Upgrades to the gamma ray imager on DIII-D enabling access to high flux hard x-ray measurements during the runaway electron plateau phase (invited),” *Rev. Sci. Instrum.* **93**, 113524 (2022).

<sup>12</sup>M. D. Rosa *et al.*, “Design solutions for the hodoscope of the magnetic proton recoil neutron spectrometer of the SPARC tokamak,” *Rev. Sci. Instrum.* **95**, 083508 (2024).

<sup>13</sup>R. M. Magee, D. J. Den Hartog, S. T. A. Kumar, A. F. Almagri, B. E. Chapman, G. Fiksel, V. V. Mirnov, E. D. Mezonlin, and J. B. Titus, “Anisotropic ion heating and tail generation during tearing mode magnetic reconnection in a high-temperature plasma,” *Phys. Rev. Lett.* **107**, 065005 (2011).